Stereospecific Reaction of Muscle Fiber Proteins with the 5′ or 6′ Isomer of (Iodoacetamido)tetramethylrhodamine†

Katalin Ajtai,* Predrag J. K. Ilich, András Ringler, Salah S. Sedarous, Daniel J. Toft, and Thomas P. Burghardt

Department of Biochemistry and Molecular Biology, Mayo Foundation, Rochester, Minnesota 55905

Received March 27, 1992; Revised Manuscript Received September 29, 1992

ABSTRACT: The labeling of muscle fiber proteins with (iodoacetamido)tetramethylrhodamine (IATR) was reinvestigated with the purified 5′ or 6′ isomers of IATR. Both isomers modify the myosin heavy chain within the 20-kDa fragment of myosin subfragment 1 (S1) but with different rates, and only the 5′-IATR alters K^+–EDTA- and Ca^{2+}-activated ATPases. Absorption spectroscopic and ATPase studies of probe stoichiometry indicate that for 5′-IATR there are two probes per myosin sulfhydryl 1 (SH1). Quantitative fluorograms of the SDS–PAGE gels confirm that there are one covalent and one noncovalent probe per SH1 when S1 is labeled with 5′-IATR (5′-IATR-S1) and that there are one covalent and two noncovalent probes per S1 when S1 is labeled with 6′-IATR (6′-IATR-S1). The 5′- and 6′-IATR probes have similar fluorescent lifetimes when bound to S1, but quenching studies with potassium iodide show that 5′-IATR-S1 has a single class of strongly bound chromophores while 6′-IATR-S1 has two or more classes of chromophores. It is possible that 5′-IATR labels SH1 as a dimer. The polarization anisotropies of 5′- and 6′-IATR-S1 indicate that 5′-IATR is immobilized, while 6′-IATR is moving independently, on the surface of S1. The emission spectrum from 5′-IATR-S1 is unaffected by the addition of MgATP, while 6′-IATR-S1 shows a spectral shift and total intensity change. When labeling muscle fibers, 5′-IATR labels myosin SH1 and differentiates between the fiber physiological states by indicating cross-bridge rotation in quantitative agreement with previous results [Burghardt et al. (1983) *Proc. Natl. Acad. Sci. U.S.A. 80,* 7515]. 6′-IATR reacts preferentially with actin in muscle fibers and does not differentiate between fiber physiological states as expected for an actin probe. The stereospecificity of the rhodamine isomers for SH1 indicates features of the local protein structure. The experimental results are used with theoretical methods for determining molecular structure to suggest a qualitative scheme for the specific interaction of 5′-IATR with its binding pocket on the surface of S1.

The mixed-isomer xanthene dye 5′- and 6′-(iodoacetamido)-tetramethylrhodamine (IATR) has had a major role in the investigation of myosin cross-bridge order and orientation. IATR modifying myosin SH1 in muscle fibers was first used to detect the rate of activated cross-bridge rotational relaxation with fluorescence polarization fluctuations (Borejdo et al., 1979). With steady-state fluorescence polarization experiments on IATR-labeled fibers we showed that the cross-bridge was able to maintain more than one actin-bound orientation and that cross-bridges in active isometric fibers are oriented differently than in rigor fibers (Borejdo et al., 1982; Burghardt et al., 1983). In subsequent work we showed that IATR-labeled cross-bridges rotate from their orientation in rigor as a result of changing temperature (Ajtai & Burghardt, 1986) or the application of negative stress (Burghardt & Ajtai, 1989).

In 1988, the principal source of IATR (Molecular Probes Inc., Eugene, OR) began to sell an IATR probe originating from a newly developed synthesis. Using the new mixed 5′ and 6′ isomer IATR on fibers, we were unable to obtain our previously reported results. We found that the new dye did not label the fiber as efficiently as the old one and that the fluorescence polarization ratios from IATR-labeled fibers did not distinguish the different physiological states of the fiber as we reported earlier (Burghardt et al., 1983; Ajtai & Burghardt, 1986). We also noticed a change in the extinction coefficient spectrum of the new 5′- and 6′-IATR and the inability of the probe to inhibit the K^+–EDTA ATPase of the modified myosin.

We investigated these phenomena by using the purified isomers on our muscle system. The structural formulas of 5′- and 6′-IATR are shown in Figure 1. We found that the results obtained with the new mixed-isomer probe are identical to those obtained from the pure 6′-IATR and that the pre-1988 results are obtained with the pure 5′-IATR. Apparently, the new mixed isomer probe contains mainly the 6′ isomer, while the old preparation was predominantly the 5′ isomer.

We show below that the properties of 6′-IATR on muscle fibers are from the tendency of the 6′ isomer to label actin rather than myosin SH1. Studies with 6′-IATR-labeled myosin subfragment 1 (6′-IATR-S1) in solution indicate that the probe differs from the 5′ isomer in that it (i) reacts less efficiently with S1, (ii) is more independently mobile on the surface of S1, (iii) has an altered fluorescence emission spectrum and additional independent mobility when 6′-IATR-S1 binds MgATP, and (iv) does not inhibit K^+–EDTA ATPase. On the other hand, the 5′-IATR probe specifically and rigidly modifies SH1 in fibers and in isolated S1 and the binding of nucleotide to the cross-bridge does not mobilize the probe or alter its local environment.

The present work also indicates some previously unknown properties of the 5′-IATR modification of myosin. We show below that the stoichiometry of the probe labeling is two probes per SH1 modification. This labeling involves one covalent and one noncovalent probe with both probes localized at SH1. Evidence suggesting that these probes at SH1 are in a highly stable dimer conformation come from studies of 5′-IATR-S1 in solution and include the observation of a single predominant

† This work was supported by the National Science Foundation (DMB88-19755), the National Institutes of Health (R01 AR39288), the American Heart Association (AHA Grant-in-Aid 900644), and the Mayo Foundation. T.P.B. is an Established Investigator of the American Heart Association.

0006-2960/92/0431-12431$03.00/0

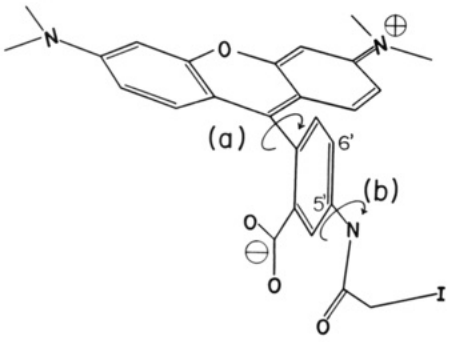

FIGURE 1: Structural formula of the dye 5′-IATR in its most probable conformation. (a), (b), and arrows indicate flexible regions of the molecule (see Results, section V).

fluorescence lifetime, a single dynamic quenching rate, and a high time-zero fluorescence anisotropy. We also show evidence for the formation of dimers in free 5′-IATR at low concentration.

The stereospecific reaction of dimers of 5′ and 6′ isomers of IATR with myosin SH1 also indicates a new aspect of the nature and size of the chromophore binding pocket at the SH1 group. We investigate the implications of our findings concerning the local protein conformation and the possible probe–probe and probe–protein interactions using methods in computational chemistry including geometry optimization for energy minimization and electron transition calculations. We develop qualitative pictures for (i) likely structure for the 5′-IATR dimer, (ii) the difference in probe–protein conformation between the 5′ and 6′ isomers when docking with the binding pocket at SH1, and (iii) possible detailed interactions between the 5′-IATR dimer and the amino acid side chains near SH1 that stabilize the dimer and prevent its independent movement.

MATERIALS AND METHODS

Chemicals. ATP, ADP, P^1,P^5-di-5′-adenosyl pentaphosphate (Ap_5A), phenylmethanesulfonyl fluoride (PMSF), ethylenediaminetetraacetic acid (EDTA), ethylene glycol bis-(β-aminoethyl ether)-*N*,*N*,*N*′,*N*′-tetraacetic acid (EGTA), dithiothreitol (DTT), iodoacetamide (IAA), 4-hydroxy-2,2,6,6-tetramethylpiperidine-1-oxyl (TEMPOL), glucose, hexokinase, and creatine kinase were from Sigma (St. Louis, MO). ^{14}C-IAA was from Amersham (Arlington Heights, IL). Thiopropyl-Sepharose 6B and activated thiol-Sepharose 4B were from Pharmacia (Uppsala, Sweden). The fluorescent labels 5′- and 6′-(iodoacetamido)tetramethylrhodamine (5′- and 6′-IATR), IUPAC nomenclature *o*-[6′-(dimethylamino)-3′-(dimethylimino)-3*H*-xanthen-9-yl]-*m*(*p*)-(β-iodoacetamido)benzoic acid, where *m* (*p*) means meta (para) and corresponds to 5′-IATR (6′-IATR), were from Molecular Probes (Eugene, OR). Urea and acrylamide were ultrapure and were from Schwartz Mann Biotechnology (Cleveland, OH). All other chemicals were analytical grade.

Solutions. In the fiber studies, rigor solution was 80 mM KCl, 5 mM $MgCl_2$, 2 mM EGTA, 1 mM DTT, and 5 mM phosphate buffer at pH 7.0. Relaxing solution was the same as rigor solution with 4 mM ATP added. In MgADP solution, 4 mM ADP was added to rigor solution together with 100 μM Ap_5A to inhibit myofibrillar myokinase from converting ADP to ATP and an ADP-regenerating system of 10 mM glucose and 0.1 mg/mL hexokinase to convert ATP to ADP. Contracting solution was the same as relaxing solution with 0.1 mM $CaCl_2$ replacing the EGTA and an ATP-regenerating solution consisting of 4 mM phosphocreatine and 0.4 mg/mL creatine kinase. Glycerol-containing solution for the low-temperature studies was rigor with 50% glycerol (v/v) at pH 7.0.

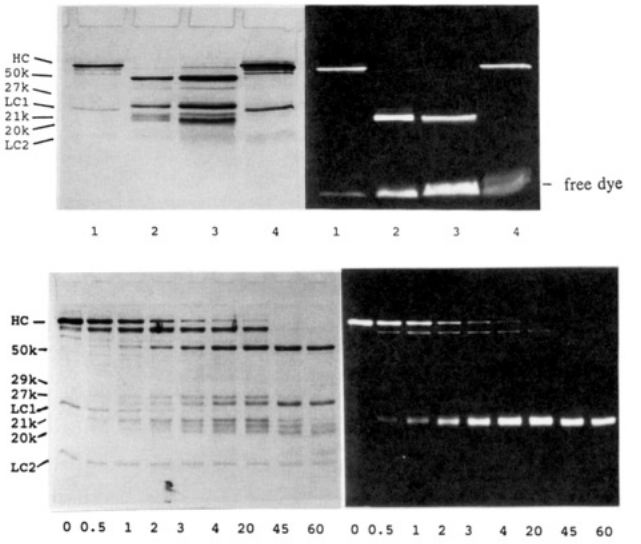

FIGURE 2: (Top) Coomassie-stained (left) and fluorescent (right) SDS–PAGE of the tryptic digestion of 5′- and 6′-IATR-S1. Lane 1, 5′-IATR-S1; lane 2, tryptic digest of 5′-IATR-S1; lane 3, tryptic digest of 6′-IATR-S1; lane 4, 6′-IATR-S1. The photograph shows the noncovalently bound dye associated with S1. (Bottom) Time course of the digestion of 5′-IATR-S1. The lanes show the time of digestion with trypsin in minutes.

Preparation and Labeling of Myosin Subfragment 1. Rabbit myosin was prepared by a standard method (Tonomura et al., 1966). S1 was prepared by digesting myosin filaments with α-chymotrypsin (Weeds & Taylor, 1975). The IATR treatment of S1 was performed in various concentrations of free dye ranging from 0.5- to 2.0-fold molar excess of the dye over the protein (corresponding to probe concentrations of 80–320 μM) in 50 mM TES buffer at pH 7.0 and 4 °C for 24 h. The reaction was stopped by separating the labeled proteins from the free dye on a Sephadex G25 column equilibrated with 50 mM TES buffer at pH 7.0. The protein was further dialyzed in the same buffer in the presence of 0.1 mM PMSF. The digestion of S1 was carried out in 50 mM Tris-HCl at pH 8.0 and 25 °C with an S1/trypsin ratio of 1:80 (Figure 2, top) or 1:50 (Figure 2, bottom) (Bálint et al., 1975, 1978).

Localization of the probes in the proteolytic fragments of S1 was carried out using sodium dodecyl sulfate–polyacrylamide gel electrophoresis (SDS–PAGE) on the tryptic digest of probe-labeled S1 (Bálint et al., 1975). Shown in Figure 2 are Coomassie-stained and fluorescent images of the SDS–PAGE experiment of labeled S1. Tryptic proteolysis of S1 produces three characteristic fragments of 50-, 27-, and 20-kilodalton (kDa) molecular masses. SH1 resides on the 20-kDa fragment (Bálint et al., 1978). We show in Figure 2 (top) that the covalently bound 5′- and 6′-IATR are localized in the heavy chain of S1 and migrate with the 20-kDa fragment of tryptic S1. The 5′-IATR-S1 showed an altered tryptic digestion profile in that we observed an additional peptide with a molecular mass of ~21 kDa. We investigated the time course of the digestion and show in Figure 2 (bottom) that the appearance of the new fragment is correlated with the disappearance of the 29-kDa fragment, indicating that the 29-kDa fragment is the precursor of the 21-kDa fragment.

We estimated the specificity and extent of modification of sulfhydryls in S1 using the characteristic alteration of myosin S1 ATPase activity whereby the specific modification of SH1

causes a linear inhibition of the K^+–EDTA and activation of the Ca^{2+} ATPase activity. Enzymatic activity was measured at 30 °C according to Ajtai et al. (1990). There were six different S1 preparations. The K^+–EDTA- and Ca^{2+}-activated ATPase activities for unlabeled S1 were 10.9 ± 1.0 and 1.2 ± 0.1 μmol of phosphate/(mg of S1·min), respectively. The changes in the ATPase activities from covalent modification of S1 with IATR are related to these control activities.

Preparation and Labeling of Muscle Fibers. We obtained rabbit psoas muscle fibers and stored them in relaxing solution containing 50% glycerol (v/v) at −15 °C for up to several weeks (Borejdo et al., 1979). We labeled the skinned fibers with 70 μM IATR in relaxing solution without DTT for 30 min at 4 °C with intensive stirring. The reaction was stopped with 1 mM DTT and the excess dye was washed out with relaxing solution (Ajtai & Burghardt, 1986).

Quantitative Absorption Measurements. We made steady-state absorption measurements on a Beckman DU70 spectrophotometer (Beckman Instruments, Fullerton, CA). The estimation of probe stoichiometry from the absorption spectrum of labeled myosin was done by comparing extinction coefficients from protein-bound and free IATR in 8 M urea. Labeled proteins were denatured in 8 M urea to disrupt the interaction between the dyes and the protein and the absorption spectrum was recorded. Free 5′- and 6′-IATR was also dissolved in 8 M urea and the absorption spectrum was recorded. The shape and peak position of the spectra were identical for the free and protein-bound dyes under this condition, suggesting that the amount of protein-bound probe could be reliably estimated by comparison of absorption spectra. We found that the extinction coefficients at the absorption maximum of 555 nm were 7.9×10^4 and 6.9×10^4 $(M \cdot cm)^{-1}$ for 5′- and 6′-IATR, respectively.

Quantitative Fluorescence Measurements. (i) Time-Resolved Fluorescence Experiments. We performed time-resolved fluorescence measurements on a pulsed laser excitation instrument with an excitation wavelength of 575 nm and an emission wavelength of 600 nm. Lamp pulse widths were ~50 ps. Emission was collected at 90° from the direction of propagation of the excitation beam. The excitation was done at the magic angle polarization condition (Hedstrom et al., 1988).

Fluorescence lifetimes for the quenching experiments were obtained from solutions of IATR and IATR-labeled S1 in 50 mM TES, pH 7.0, and T = 14 °C with KCl concentration adjusted to keep ionic strength at 0.2 M. The fluorescence lifetime decay curves were well fitted by a method described previously using a sum of two exponentials with amplitudes α and fluorescence lifetimes τ (Burghardt & Ajtai, 1986).

(ii) Time-Independent Fluorescence Experiments. We performed steady-state fluorescence measurements on a SLM 8000 spectrofluorometer (SLM Instruments, Urbana, IL). Emission spectra from labeled S1 were recorded with an excitation wavelength of 550 nm and monochromator slits (both excitation and emission) of 1 nm.

In the fiber studies we oriented the fiber axis so that it was perpendicular to the propagation directions of both the excitation and collected emission beams. A steady-state fluorescence polarization experiment consisted of collecting the fluorescence intensities $F_{\parallel,\parallel}$, $F_{\parallel,\perp}$, $F_{\perp,\parallel}$, and $F_{\perp,\perp}$ from IATR-modified fibers as a function of excitation wavelength. The first (second) index of F corresponds to the direction of the linear polarization of the excitation (emission) beam. Parallel (∥) and perpendicular (⊥) are directions relative to the fiber axis. These intensities have identical but arbitrary

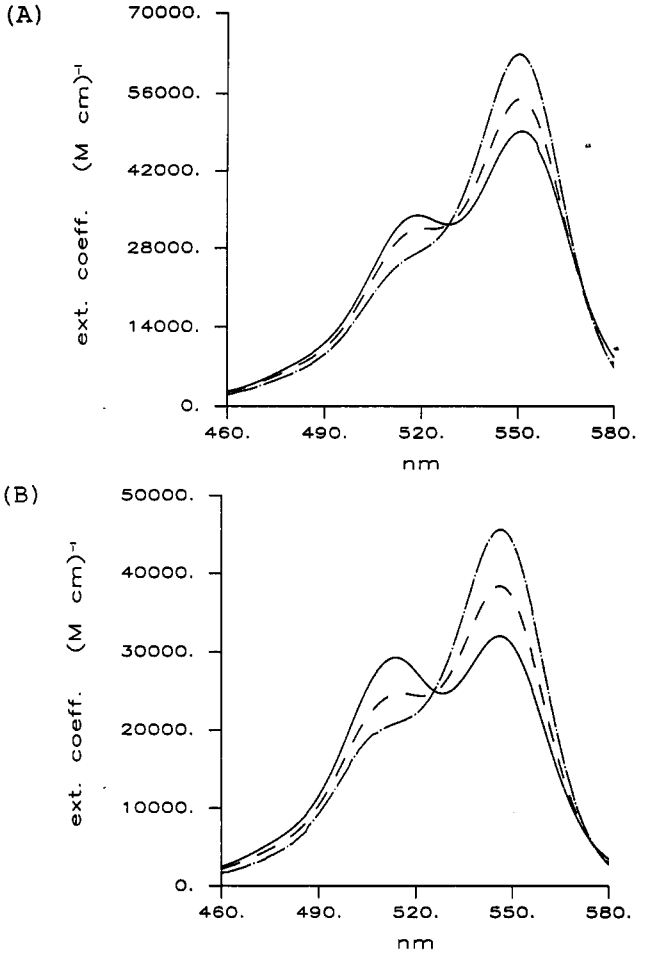

FIGURE 3: Extinction coefficient spectra of 5′-IATR (A) and 6′-IATR (B) showing the concentration dependence of the effective extinction coefficient, ε. Absorption spectra were recorded for initial concentration of 5′-IATR probes of $[M]_0$ = 500 μM (—), 100 μM (– – –), and 10 μM (– · –), with path lengths of 0.1, 0.2, and 1.0 cm, respectively. For 6′-IATR, $[M]_0$ = 500 μM (—), 50 μM (– – –), and 5 μM (– · –), with path lengths of 0.1, 1.0, and 1.0 cm, respectively. The anomaly at λ = 558 nm is due to an incorrect baseline correction in the software of the absorption spectrometer.

normalization so they were combined into three ratios:

$$P_{\parallel} = \frac{F_{\parallel,\parallel} - F_{\parallel,\perp}}{F_{\parallel,\parallel} + F_{\parallel,\perp}} \qquad P_{\perp} = \frac{F_{\perp,\perp} - F_{\perp,\parallel}}{F_{\perp,\perp} + F_{\perp,\parallel}}$$

$$Q_{\parallel} = \frac{F_{\parallel,\parallel} - F_{\perp,\parallel}}{F_{\parallel,\parallel} + F_{\perp,\parallel}} \qquad (1)$$

We plotted $P_{\parallel}$, $P_{\perp}$, and $Q_{\parallel}$ as functions of excitation wavelength, λ_{ex} (slits at 4 nm). The emission wavelength, λ_{em}, was selected with a band-pass filter giving λ_{em} = 570 ± 10 nm.

Computation of Molecular Structures. We preformed geometry optimization of IATR and peptide fragments of S1 by the semiempirical quantum methods MNDO (Dewar & Theil, 1977) and AM1 (Dewar et al., 1985). Energy minimization and calculation of electron densities of the smaller fragments were carried out by the ab initio method GAUSSIAN-90 (Frisch et al., 1990), with a basis set ≥ 4-31G*. Calculation of electronic transition properties was carried out by the INDO/1S-CI method (Ridley & Zerner, 1973).

RESULTS

(I) Dimer Formation in 5′- and 6′-IATR. Panels A and B of Figure 3 indicate the wavelength and concentration

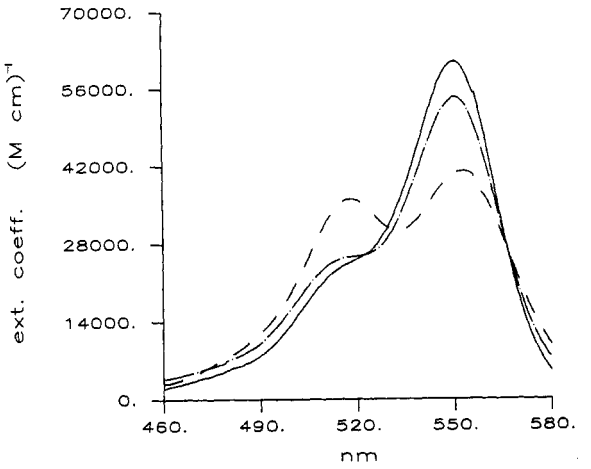

FIGURE 4: Extinction coefficient spectra of 5′-IATR monomer, ϵ_M (– · –), and dimer, $\epsilon_D/2$ (– – –), calculated from eq 3 as described in the text, compared with 5′-IATR-S1 (—). The 5′-IATR-S1 spectrum is blue-shifted 4 nm to allow its absorption maximum to coincide with that from ϵ_M. The spectra correspond to equal energy (the area of the spectrum in the frequency domain) over the wavelength domain shown. The anomaly at $\lambda = 558$ nm is due to an incorrect baseline correction in the software of the absorption spectrometer. This anomaly shows up in ϵ_M and ϵ_D because they are calculated using the observed absorption spectrum normalized for probe concentration and light path length.

dependence of the absorption spectrum divided by initial dye concentration $[M]_0$ and light path length (i.e., the effective extinction coefficient) of 5′- and 6′-IATR in 5 mM phosphate buffer at pH 7. The shape of the spectra depends on dye concentration indicating dimer (or higher aggregate) formation in both the 5′ and the 6′ isomer (Selwyn & Steinfeld, 1972; Grajek et al., 1986; Cheng & McPhie, 1989; Blonski, 1991). We modeled the dye interaction as the bimolecular reaction

$$M + M \underset{k_2}{\overset{k_1}{\rightleftarrows}} D \qquad (2)$$

where M is a monomer and D is a dimer (Rohatgi & Mukhopadhyay, 1971; Blonski, 1991). At equilibrium the effective extinction coefficient is given by

$$\epsilon = ([M]_{eq}\epsilon_M + [D]_{eq}\epsilon_D)/[M]_0 \qquad (3)$$

where ϵ_M and ϵ_D are the extinction coefficients of the monomer and dimer, respectively, $[M]_{eq} = ([D]_{eq}/K)^{1/2}$, $[D]_{eq} = {}^1/_2[M]_0\{1 + [1 - (1 + 8K[M]_0)^{1/2}]/(4K[M]_0)\}$, and the equilibrium constant $K = k_1/k_2$. We measured ϵ at three different concentration of $[M]_0$ to generate three equations of the form of eq 3, to solve for K, ϵ_M, and ϵ_D for either the 5′ or the 6′ isomer. We found that $K = (7.3 \pm 0.2) \times 10^3$ M^{-1} and $(1.8 \pm 0.1) \times 10^4$ M^{-1} for the 5′ and the 6′ isomers, respectively. Shown in Figure 4 are ϵ_M and $\epsilon_D/2$ for the 5′ isomer. Similar plots were calculated for the 6′ isomer (data not shown).

The extinction coefficient spectrum of 5′-IATR-S1 in the visible region has a maximum at 555.5 nm that is slightly red-shifted relative to the free probe in aqueous buffer (maximum at 551 nm). A qualitative comparison of the 5′-IATR-S1 spectrum with the calculated ϵ_M spectrum, made by shifting the maximum of 5′-IATR to correspond to the maximum of ϵ_M, is also shown in Figure 4. The two spectra have equal integrated energies over the wavelength region plotted. The spectrum of 5′-IATR-S1 shows a shoulder on the low-wavelength side of the maximum, suggesting the presence of the dimer species of 5′-IATR; however, comparison

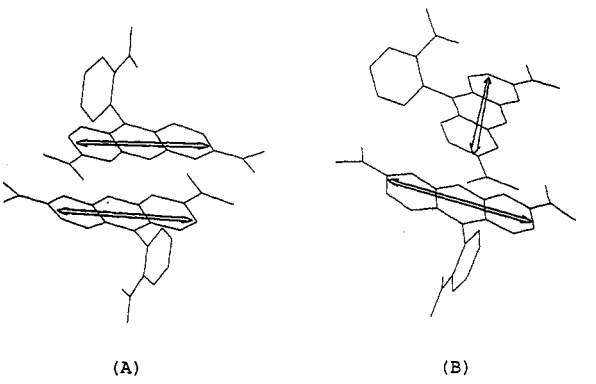

FIGURE 5: Possible modes of rhodamine association: (A) the xanthene rings are coplanar and approximately aligned along the long ring axis and (B) the rings are coplanar but the long axes (as well as the transition moment vectors) are nearly perpendicular. The iodoacetamido substituents are omitted for clarity.

with ϵ_M and ϵ_D indicates that the protein-bound probe is a mixture of monomers and dimers or a homogeneous population of probes with extinction coefficient different from both ϵ_M and ϵ_D.

Assuming for the moment that a dimer of 5′-IATR modifies S1, then what is the dimer conformation causing the observed peak shift in the absorption spectrum relative to the free dye? The amount and sign of the shift depends on the size and relative orientation of the monomer transition moments, m, and the distance, R, between the moments (Longuett-Higgins & Murrell, 1955). For the "parallel" dimer coordination, Figure 5A, a new higher energy band would occur in the absorption spectrum. Given the predicted m of 4.5–5.5 D and a van der Waals interaction distance of 3.8–4.2 Å, a new band blue-shifted 1200–1800 cm^{-1} is predicted for the parallel dimer. For the "perpendicular" association, Figure 5B, the very weak coupling of moments produces a very small red shift. It happens that the observed shoulder at 518 nm (Figure 4) is 1160 cm^{-1} blue-shifted with respect to the principal band at 551 nm, indicating a preference for the parallel coordination.

(II) Specificity and Stoichiometry of 5′- and 6′-IATR in Myosin S1. S1 was labeled with various amounts of the IATR isomers and we estimated the amount and location of incorporation of the dye into S1 by light absorption, SDS–PAGE, and ATPase measurements. We summarize the results in Table I.

(A) Absorption Measurements. We estimated the mol/mol ratio of dye incorporation in S1 by absorption using the method described in Materials and Methods. S1 was labeled with treating solutions ranging from 0.5:1 to 2.4:1, dye/S1, as indicated in column 1 of Table I. The incorporation of the dyes into S1, indicated in column 2 of Table I, was approximately linear with the treating dye concentration. 5′-IATR labels S1 about twice as effectively as 6′-IATR.

(B) ATPase Measurements. The inhibition and activation of the ATPases by probe modification of S1 were measured as the percentage relative to unmodified S1 (see Table I). With 5′-IATR, both the inhibition of the K$^+$–EDTA ATPase (column 3) and the activation of the Ca^{2+} ATPase (column 4) are linearly related with the mol/mol incorporation of dye estimated by absorption, as indicated in Figure 6. Ca^{2+} vs K$^+$–EDTA ATPases is linear for 5′-IATR up to ~50% modification of SH1, in close agreement with other specific probes of SH1 (Ajtai et al., 1990). This result demonstrates a strong correlation between modification of SH1 and the amount of dye molecules per protein, suggesting that 5′-IATR is a specific label of SH1. We checked the accuracy of the

Table I: Binding Stoichiometry of 5′- and 6′-IATR on S1

molar ratio of dye/protein treatment	molar ratio of dye/protein incorporated	ATPases[a]		5′-IATR/SH1 stoichiometry[b]	fraction of free SH1	dye distribution calcd from SDS–PAGE (%)	
		K^+–EDTA inhibition	Ca^{2+} activation			protein-bound	free
5′-IATR							
0.5:1	0.34	0.16	2.22	2.12			
1.0:1	0.64	0.30	3.23	2.00	0.64[c]	45	55
1.2:1	0.88	0.41	3.40	2.07			
2.0:1	1.04	0.58	5.61	1.79			
2.0:1[d]	0.38	1.00	4.15		0.00[e]	46	54
6′-IATR							
1.2:1	0.30	0	1.30			36	64
1.5:1	0.40	0	1.45				
2.4:1	0.87	1.25[f]	1.78			36	64

[a] Given as percentage relative to unmodified S1. [b] The stoichiometry of the 5′ isomer for SH1 modification was estimated by dividing the total amount of probe per S1 (estimated by absorption; column 2) by the fraction of covalently modified SH1s (estimated by inhibition of K^+–EDTA ATPase; column 3). [c] Measured with ^{14}C-IAA. [d] Pretreated with IAA. [e] Measured with K^+–EDTA ATPase (18% free SH1 after reaction with IAA). [f] K^+–EDTA ATPase is activated.

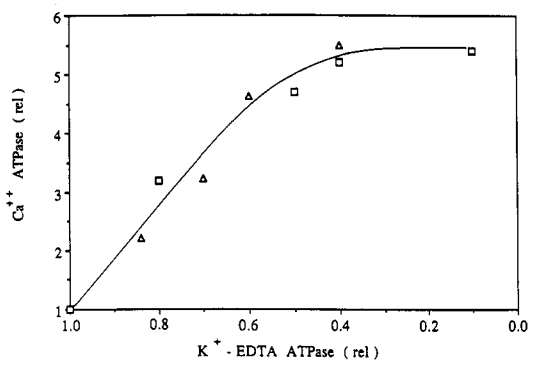

FIGURE 6: Ca^{2+} vs K^+–EDTA ATPase for 5′-IATR-S1 (△). The linear region corresponds to the specific modification of SH1. Similar measurements for iodoacetamido-TEMPO spin label (ITSL) labeling S1 (□) is shown for comparison [data taken from Ajtai et al. (1990)].

K^+–EDTA ATPase for estimating the fraction of SH1 modification by measuring the amount of available SH1s after reaction with 5′-ITAR by using ^{14}C-IAA. The sum of the fractions corresponding to SH1 modification with either 5′-IATR (row 2, column 3) or ^{14}C-IAA (row 2, column 6) gives 0.94, in close agreement with the expected sum of 1.0. In contrast, 6′-IATR does not inhibit K^+–EDTA ATPase.

The stoichiometry of the 5′ isomer for SH1 modification was estimated by dividing the total amount of probe per S1 (estimated by absorption) by the fraction of covalently modified SH1s (estimated by inhibition of K^+–EDTA ATPase). This result is reported in Table I (column 5). We find that within the linear region of Figure 6 there are two 5′-IATR molecules per modified SH1. The stoichiometry of 6′-IATR for SH1 modification could not be estimated by this method because the reaction of 6′-IATR with S1 does not affect K^+–EDTA ATPase.

The two probes per SH1 stoichiometry of 5′-IATR could be explained by the existence of a nonspecific binding site for 5′-IATR that binds the probe in a linear relationship with probe concentration in the treating solution. This possibility was investigated by pretreating S1 with IAA to specifically modify 82% of the SH1s (determined by K^+–EDTA ATPase) and then treating the S1 with a high concentration of 5′-IATR. If a nonspecific site for 5′-IATR exists, then under these conditions we would expect a probe per SH1 stoichiometry of ~6.6. This experiment, reported in row 5 in Table I, shows that the remaining 18% of SH1s bind 0.38 5′-IATR/SH1, giving a probe per SH1 stoichiometry of 2.1. This evidence again suggests that a 5′-IATR dimer modifies SH1.

The reaction of 6′-IATR with S1 is weaker than with 5′-IATR in that under identical labeling conditions fewer 6′-IATRs label S1 than 5′-IATRs.

(C) SDS–PAGE Measurements. The specificity and stoichiometry of the 5′ and 6′ isomers for S1 were estimated using SDS–PAGE (see Figure 2) and quantitative fluorescence gel scanning. Columns 7 and 8 of Table I summarize our findings. We followed the migration of the fluorescent probes with myosin S1 and proteolytic fragments of S1. For both isomers the probe modified the heavy chain of myosin and the 20-kDa proteolytic fragment of the heavy chain. A significant amount of free dye was also detected for both isomers. The amount and location of dye in the gels was estimated by fluorescence gel scanning. For 5′-IATR modifying S1, the amount of free dye equaled the amount of protein-bound dye, consistent with a 5′-IATR dimer modifying SH1 in S1. For 6′-IATR modifying S1, the amount of free dye was approximately 2 times the amount of bound dye.

(D) Tightness of Binding of the Second Probe. We tried different methods in native and denaturing conditions to remove the noncovalent 5′- and 6′-IATR from the S1. Sephadex G25 chromatography, prolonged dialysis, gel filtration in 1% SDS, and affinity chromatography using activated thiol-Sepharose 4B or thiopropyl-Sepharose 6B failed to remove the noncovalent dye from labeled S1. We dissociated the noncovalent dye by washing the trichloroacetic acid precipitate of S1 with methanol or by electrophoresis in the presence of SDS. Other iodoacetamido-based fluorescent probes modifying S1 or fibers, including dansyl, fluorescein, eosin, and erythrosin, failed to produce a significant free dye fraction, indicating that no covalent bond was reduced under these conditions. Apparently the noncovalent dye is very strongly associated with the protein and is protected by the native structure of the S1.

(III) Fluorescence Spectroscopy on 5′- and 6′-IATR on S1: (A) Fluorescence Quenching of Free and Protein-Bound Probes. When each fluorophore in a sample is equally accessible to the quencher, then a linear Stern–Volmer plot corresponding to a constant quenching rate is expected. A sample containing probes bound to different sites on a protein may have different accessibilities to the quencher and a nonlinear Stern–Volmer plot such that the quenching rate is a function of quencher concentration (Lakowicz, 1983). We performed fluorescence quenching studies on free and protein-bound probes.

We measured the lifetime of 5′- and 6′-IATR alone and when modifying S1, in the presence and absence of quenchers

Table II: Fluorescence Lifetimes of 5′- and 6′-IATR Free in Solution and When Modifying S1[a]

	τ_1	α_1	τ_2	α_2
5′-IATR	0.070 ● 0.020	0.259 ± 0.007	2.600 ± 0.020	0.741 ± 0.006
5′-IATR-S1	1.060 ● 0.500	0.040 ± 0.020	4.040 ± 0.080	0.960 ± 0.020
6′-IATR	0.070 ± 0.004	0.257 ± 0.010	2.600 ± 0.005	0.743 ± 0.010
6′-IATR-S1	0.176 ± 0.003	0.055 ± 0.004	3.800 ± 0.008	0.945 ± 0.004

[a] Experiments were performed at T = 14 °C in 50 mM TES buffer, pH 7. Fluorescence intensity curves, $F(t)$, were fitted using the expression $F(t) = \alpha_1 \exp(-t/\tau_1) + \alpha_2 \exp(-t/\tau_2)$, where lifetimes, τ_i are given in nanoseconds. Error is standard deviation.

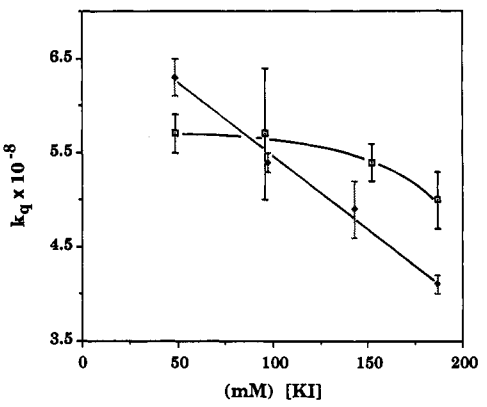

FIGURE 7: Quenching rate, k_q, as a function of the concentration of the quencher KI for 5′-IATR-S1 (□) and 6′-IATR-S1 (◆). For 5′-ITAR-S1, k_q is nearly independent of [KI], indicating a single class of quenchable probes. For 6′-IATR-S1, k_q is dependent on [KI], indicating that at least two classes of probes exist such that one class is more easily quenched.

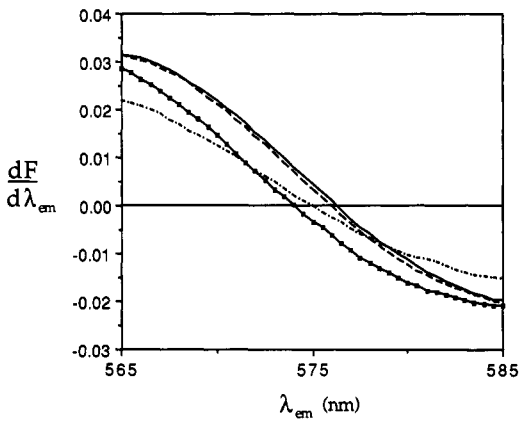

FIGURE 8: Effect of nucleotide binding to S1 on the emission spectra of 5′- and 6′-IATR-S1. The first derivatives of the emission spectra are shown from 5′-IATR-S1 in rigor buffer (—) and in the presence of MgATP (- - -) and from 6′-IATR-S1 in rigor buffer (–·–) and in the presence of MgATP (■).

to investigate the possibility that the noncovalent IATR on S1 was bound to S1 in a site other than SH1. We tried to quench the probe in solution and when protein-bound with acrylamide, TEMPOL, or KI. Only KI proved to be an effective quencher. In all cases, both isomers had two lifetimes and only the longer lifetime was altered by the presence of the quencher as observed in fluorescein-labeled S1 (Aguirre et al., 1986). In the absence of KI, the lifetimes of 5′-IATR, 6′-IATR, 5′-IATR-S1, and 6′-IATR-S1 are summarized in Table II. The lifetime of the protein-bound probe is much longer than that of the free probe, indicating that it is protected by the protein structure. With either probe modifying S1, in the absence of quencher, the longer lifetime corresponded to ≥95% (time-integrated intensity) of the total light.

In the presence of KI, the longer lifetime component of 5′- and 6′-IATR was quenched with a rate, k_q, calculated using the Stern–Volmer equation (Lakowicz, 1983). We found that $k_q = (4.73 \pm 0.08) \times 10^9$ $(M \cdot s)^{-1}$ and $(3.70 \pm 0.20) \times 10^9$ $(M \cdot s)^{-1}$ for 5′- and 6′-IATR, respectively. The k_qs for the probes are independent of quencher concentration, [KI], indicating a single class of probe that is readily accessible to quenching by KI. In the presence of KI, the longer lifetime component of 5′- and 6′-IATR-S1 was quenched with a rate summarized in Figure 7. These data show that, for 5′-IATR-S1, k_q is nearly constant and equals $(5.3 \pm 0.2) \times 10^8$ $(M \cdot s)^{-1}$ over the range of [KI] indicated, while for 6′-IATR-S1, k_q varies with [KI]. For 5′-IATR-S1, the two probes per protein behave as a single probe in their accessibility to quenchers, suggesting that they are both localized at SH1. The accessibility of the multiple 6′-IATR probes per S1 appears to be heterogeneous, suggesting that probes reside on at least two different sites on the S1.

(B) Effect of Nucleotide on Fluorescence Intensity, Polarization, and Lifetime. Shown in Figure 8 is the derivative of emission intensity as a function of wavelength from 5′- and 6′-IATR-labeled S1 in the presence and absence of MgATP. The spectra shown are on a small domain of emission wavelengths near the emission intensity maximum. These plots indicate peak emission intensity spectral differences as shifts in the zero crossing point and total intensity differences as differing slopes. The fluorescence intensity of 5′-IATR-S1 is slightly affected by the binding of MgATP. The peak position and total intensity of 6′-IATR-S1 are substantially affected by MgATP binding to the S1. Fluorescence intensity changes indicate a change in the local environment of the probe, suggesting that 5′-IATR remains fixed on the surface of S1 while 6′-IATR alters its orientation or mobility on S1 upon nucleotide binding.

Shown in Figure 9 are the steady-state excitation polarization anisotropies, $r(\lambda_{ex})$, of 5′- and 6′-IATR-S1 in rigor buffer at 4 °C and in 50% glycerol at −15 °C. The anisotropy at low temperature and in the presence of glycerol, where the probe is immobilized on the time scale of the fluorescent lifetime, indicates the angle between the absorption and emission dipoles in the molecule (Lakowicz, 1983). The two immobilized isomers have similar excitation polarization anisotropies. In rigor buffer the mobility of 6′-IATR-S1 is clearly larger than that of 5′-IATR-S1 since $|r(5'\text{-IATR-S1})| \geq |r(6'\text{-IATR-S1})|$. The steady-state polarization anisotropy spectrum for 5′-IATR-S1 in relaxing solution is identical to its spectrum in rigor solution, while for 6′-IATR-S1 there is a slight decrease in the peak polarization in relaxing solution (data not shown).

The comparison of the peak anisotropy from 5′- or 6′-IATR-S1 in rigor or relaxing solution with that from immobilized probe reflects principally the independent motion of the probe on S1 because S1 rotational relaxation can contribute only ~5% of the depolarization during the 4.0–4.4-ns lifetime of the probe. The anisotropy decrease from the independent probe movement is equivalent to allowing the probe to move rapidly (compared to the lifetime) through an angle of 10° for 5′-IATR-S1 and 21° or 22° for 6′-IATR-S1 in rigor or relaxing solution (Lakowicz, 1983). The independent mobility

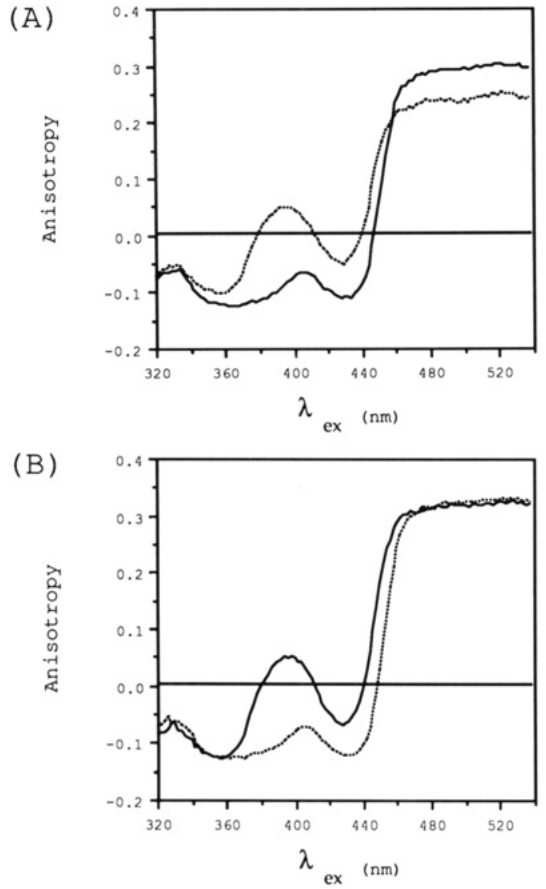

FIGURE 9: Polarization anisotropy, r, from 5′-IATR-S1 (—) and 6′-IATR-S1 (- - -) in rigor buffer at 4 °C (A) and in rigor buffer + 50% glycerol at −15 °C (B).

of 5′-IATR on S1 is very similar to that observed for fluorescein-labeled S1 (Ajtai & Burghardt, 1992).

We used time-resolved fluorescence methods to investigate lifetime and anisotropy of probe-modified S1 in rigor and in the presence of nucleotides. Our findings confirm the steady-state results, indicating that the 6′ isomer is highly independently mobile on the surface of S1 and interacts directly with nucleotides when they are present while the 5′ isomer is rigidly bound to S1 and not affected by the presence of nucleotides.

(IV) Studies of Labeled Muscle Fibers: *(A) Specificity of 5′- and 6′-IATR for Myosin SH1 in Fibers*. We studied the specificity of the rhodamine isomers in muscle fibers with protein extracts from the labeled fibers. We identified the fluorescent components of the samples under UV excitation light. We also performed a quantitative estimation of the distribution of fluorescence by fluorescence gel scanning, and the results are summarized in Figure 10. While 5′-IATR reacted predominantly with the myosin heavy chain, 6′-IATR had lower reactivity with the muscle proteins and labeled predominantly actin. Also visible in the gel is the free dye originating from the noncovalent partner of the rhodamine dimer at SH1.

(B) Fluorescence Polarization of 5′- and 6′-IATR-Labeled Fibers. Figure 11 shows the fluorescence polarization spectra from 5′- and 6′-IATR-labeled fibers in four different physiological conditions. We find that only the 5′-IATR probe gives polarization ratios that differentiate each of the physiological states of the fiber and that are in agreement with previous measurements of the polarization ratio, $P_\perp$, using the mixed-isomer probe (Ajtai & Burghardt, 1986). The 6′-IATR probe gives polarization spectra that are insensitive to

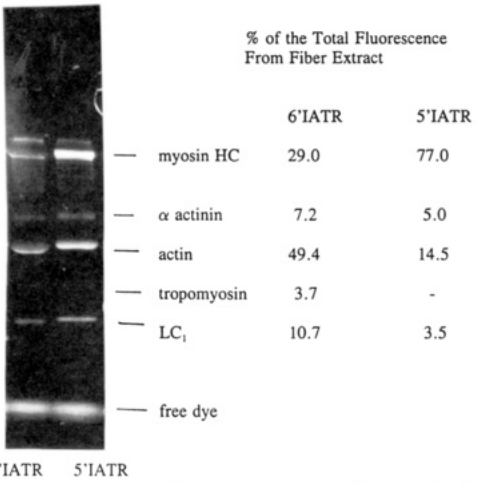

FIGURE 10: Specificity of 5′- and 6′-IATR for myosin in muscle fibers: SDS–PAGE of 6′-IATR- (lane 1) and 5′-IATR- (lane 2) labeled muscle fiber protein extrract. IATR incorporation is expressed as the percentage of the total protein-bound fluorescence observed in the gel.

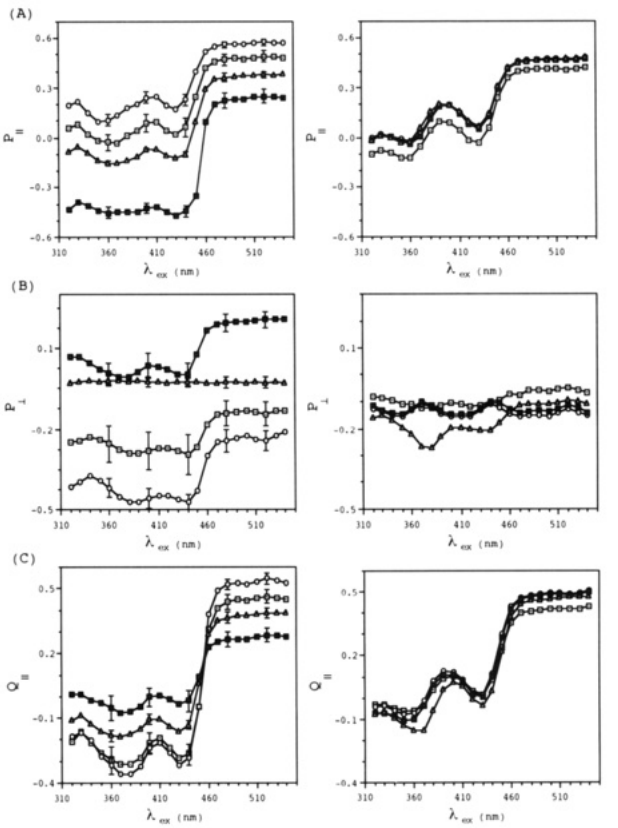

FIGURE 11: Fluorescence polarization ratios $P_\parallel$ (A), $P_\perp$ (B), and $Q_\parallel$ (C) from 5′-IATR- (left) and 6′-IATR- (right) labeled muscle fibers in rigor (■), in relaxation (△), in the presence of MgADP (○), and in isometric contraction (□). Error bars represent standard deviation.

the physiological state of the fiber and different than previous results using the mixed-isomer probe.

(V) Calculation of Molecular Conformation. There are two flexible domains in the 5′-IATR label: (a) the bridge bond between the xanthene and benzene rings and (b) the bonds between the dye–protein tether; see Figure 1 (a) and (b). In the crystalline phase, the xanthene and benzene rings are perpendicular when in complex with heavy metals (Thorn & Fultz, 1989; Abrams et al., 1986). The same conformation is predicted by most of our geometry optimization calculations of the 5′-IATR–Cys complex in vacuo, although the rings can

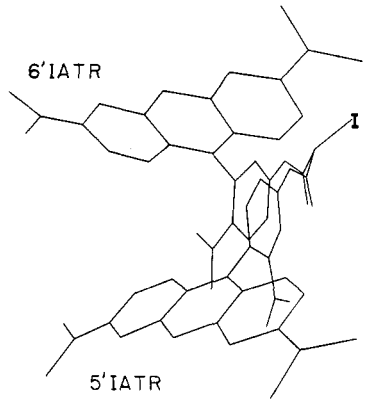

FIGURE 12: The 5′ and 6′ isomers in stable conformations with aligned terminal C–I bonds.

rotate 15–20° within a 5 kcal/mol energy barrier. Given that the imino and amino groups are indistinguishable, due to tautomeric exchange, this conformation would have a symmetry plane bisecting the xanthene ring. The acetamido–cysteinyl domain is predicted by our calculations to be coplanar with the benzene ring. In a free dye parts of this domain rotate through a full circle with energy barriers of 2–8 kcal/mol so that thermal excitation at room temperature is unlikely to induce large variability in the conformation of the rhodamine probe. The observed high polarization in the fluorescence spectra suggests that the 5′-IATR probe is more firm in the complex with S1 at SH1 than the calculations of a free dye conformation would imply.

Far more pronounced and with seemingly larger consequences are the structural differences between the 5′ and 6′ isomers of the rhodamine probe. Computer-simulated docking of the probe with a cysteine, shown in Figure 12, indicates that the positions of the dimethylamino groups on the xanthene rings in the two isomers can differ by as much as 20 Å relative to the same joining point with S1. It is plausible that the markedly higher specificity of the 5′ isomer originates from a better steric fit to the SH1 domain of the S1 protein.

DISCUSSION

(I) Specificity, Rigidity, and Stoichiometry of 5′- and 6′-IATR. We presented data indicating the specificity, rigidity, and stoichiometry of the 5′- and 6′-IATR derivatives for myosin S1 and the myosin cross-bridge in muscle fibers. Considering first the question of the specificity of the probes, we determined that 5′-IATR specifically modifies SH1 since it migrates with the 20-kDa proteolytic fragment of S1 in SDS–PAGE and because it causes the alteration of the myosin ATPases characteristic of specific SH1 modification. 6′-IATR is less reactive with S1 than 5′-IATR, and whether or not 6′-IATR modifies SH1 in S1 is uncertain since, although the probe migrates with the 20-kDa proteolytic fragment of S1 in SDS–PAGE, the K^+–EDTA ATPase is unaffected. The tryptic digestion of 6′-IATR-S1 shows a regular digestion pattern since fragments of 27, 50, and 20 kDa are formed (Bálint et al., 1975). In contrast, in the digest of 5′-IATR-S1 we observed the formation of an additional fragment of 21 kDa from a 29-kDa precursor (see Figure 2, bottom). A similar fragment, also formed from the 29-kDa precursor, was observed previously from S1 digestion (Muhlrad & Hozumi, 1982; Mócz et al., 1984). The altered proteolysis shows an effect on protein structure due to modification with rhodamine.

On the question of probe rigidity, we showed that 5′-IATR is more rigidly bound to S1 than 6′-IATR since time-resolved

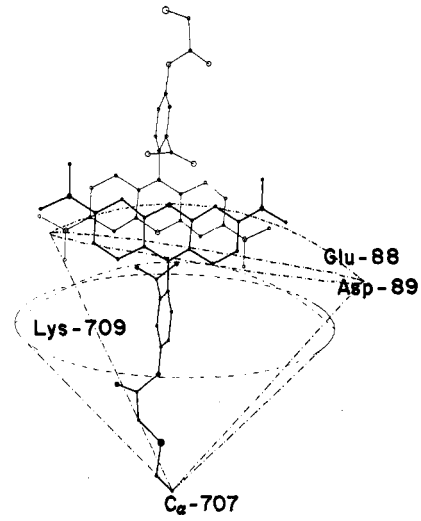

FIGURE 13: Model of the 5′-IATR dimer attached to Cys 707 of S1. The spherical surface of the smaller cone of diameter 10.5 Å represents the possible positions of the negatively charged carboxyl group on the benzene ring. The spherical surface of the large cone of diameter 14.5 Å represents the possible positions of the charged imino group on the xanthene. The actual location of these charged groups is not independent and is more restricted than that indicated by the spherical surfaces.

and steady-state fluorescence anisotropy indicates more independent probe movement in 6′-IATR-S1. When MgATP binds to probe-modified S1, the steady-state emission from 5′-IATR-S1 is unchanged while emission from 6′-IATR-S1 changes both intensity and wavelength maximum.

Finally, on the matter of the stoichiometry of binding of the probes, we showed that there are two 5′-IATR molecules per S1 or three 6′-IATR molecules per S1. Different rhodamine derivatives and other xanthene dyes have a well-known tendency to form dimers or higher aggregates (Rohatgi & Mukhopadhyay, 1971; Selwyn & Steinfeld, 1972; Cheng & McPhie, 1989; Grajek et al., 1986; Thorn & Fultz, 1989; Blonski, 1991; López Arbeloa et al., 1991) and we determined that the 5′- and 6′-IATR molecules are not exceptional in this matter. The stoichiometry of the 5′ isomer at SH1 is firmly established as two probes per SH1 by comparing the amount of light absorption of the dye to the inhibition of the K^+–EDTA ATPase. The ratio of two probes per SH1 is maintained in samples where the percent of S1s modified ranges from 18% to 100%, ruling out the possibility that the noncovalent probe was attached to S1 at a site other than SH1. Furthermore, quantitative fluorescence gel scanning detects an equal amount of free and 20-kDa-bound probe from digested S1 applied to SDS–PAGE gels. The two 5′ isomers are tightly trapped by the native protein structure with a very high affinity.

(II) Interaction of 5′-IATR with the SH1 Region of S1. There are apparently three domains in the dye molecule likely to interact with S1: (i) the highly polar amido group in the rhodamine–protein link, (ii) the electron-rich carboxyl group on the benzene ring, and (iii) the electron-deficient dimethylimino group on the xanthene ring; see Figures 1 and 13. The carboxyl group is ionized at neutral pH and can rotate and bend around the bonds shown in Figure 1. Within a 2–8 kcal/mol energy barrier, the carboxyl group can appear anywhere on the surface of the spherical surface of the smaller cone of 10.5-Å diameter in Figure 13. Coulombic attraction to a proximal electron-deficient nitrogen of the Lys-709 residue (Tong & Elzinga, 1983) would suffice to keep the carboxyl group, the benzene ring, and the amido-Cys part of the dye–protein tether effectively immobile within the SH1 domain.

Immobilization of the xanthene ring, critical for the usefulness of rhodamine as a spectroscopic label, is likely to depend more on electron exchange and ring-stacking interactions than on coulombic attraction. The formally positive imino nitrogen, Figure 1, is shown by our electronic structure calculations to be slightly electron deficient. Furthermore, the dye exists in at least two tautomeric forms and the electron-deficient center exchanges rapidly across the xanthene ring, rendering the two dimethyl nitrogen substituent groups chemically equal. It is the whole xanthene ring, rather than a localized charged center in it, that will interact with an electron-rich protein group. Within a 2–8 kcal/mol barrier, the center of the ring can assume any position on the surface of the larger cone of 14.5-Å diameter shown in Figure 13.

The topography of S1 (Botts et al., 1989), coarsely mapped by cross-linking studies, indicates two groups proximal to Cys-707: the Glu-88 and Asp-89 residues in the 25-kDa fragment of S1 (Lu & Wong, 1989). Both are likely to be ionized ($pK_A \sim 4$) and therefore are electron-rich and within the reach of the xanthene ring. It is tempting to suggest that a synergism of the electron attraction and electron exchange interactions among the four bodies, rhodamine, Lys-709, Glu-88, and Asp-89, is responsible for the specificity of 5′-IATR for the SH1 site and its immobility on the protein. Were the rhodamine self-associated to form a head-to-head xanthene ring stack, as found by X-ray structural studies of rhodamine–heavy metal complexes and suggested by our optical spectroscopic data, then the effective distance between the xanthene rings and Glu-88 and Asp-89 residues could be significantly shorter. It is likely that a rhodamine dimer is a stable, diamagnetic species with a strong electron deficiency across the xanthene ring stack. A tight coordination of the latter with a complementary negative center would reduce the rotational flexibility of the xanthene ring. The carboxyl group and iodine of the noncovalent member of a dimer linked to SH1 are shown in Figure 13. This carboxyl group would be positioned 21–23 Å away from Cys-707 and may interact with another charged group on S1. The unusual stability of the 5′ isomer may be due to the dimer's ability to form two points of contact with charged groups on the surface of S1.

(*III*) *Does a Dimer Modify SH1*? The conformation of 5′-IATR when it modifies SH1 in cross-bridges remains unclear. The two 5′-IATR probes on SH1 behave as a single probe from the point of view that they have a single predominant lifetime, a quenching rate independent of quencher concentration, and a high time-zero anisotropy. This evidence suggests that the 5′-IATR probe is a dimer when associated with SH1. The extinction coefficient spectrum of 5′-IATR-S1 does not strongly support this conclusion because it more closely resembles the monomer extinction coefficient, ϵ_M, than the dimer coefficient, ϵ_D; see Figure 4. There is no strong argument that implies, however, that ϵ_M from free 5′-IATR is a reasonable approximation for that from the molecules bound to SH1. It is possible that the conformation of a dimer of 5′-IATR in solution is perturbed by its interaction with amino acid side chains in the vicinity of SH1, when this molecule modifies SH1. The association constant of 5′-IATR in solution is large enough that a substantial amount of dimers are contained in the labeling solutions of S1 and intact fibers. Thus the mechanism of the modification of SH1 by 5′-IATR may involve the dimer directly or the association of a monomer with SH1 and subsequent dimer formation.

(*IV*) *Muscle Fiber Studies*. The clearest and most important difference between the 5′- and 6′-IATR molecules is provided by the intact fiber system, where 5′-IATR specifically and rigidly modifies SH1 on myosin cross-bridges and reports orientation changes due to changing physiological states of the fiber, as reported previously (Burghardt et al., 1983; Ajtai & Burghardt, 1986). In contrast, 6′-IATR labels both actin and myosin, does not sense changes in cross-bridge orientation, and is independently mobile on the surface of myosin. This result clarifies certain contradictions about the use of IATR as a muscle fiber label. The results of Tanner et al. (1992), that the probe interacts directly with nucleotides associated with the cross-bridge, very likely originate from the 6′-IATR label. In that work the difference in the dichroic signal between fibers in rigor and in the presence of MgADP is 0.166 (–0.120 → 0.046), while in our previous work this difference was 0.45 (–0.28 → 0.17) (Burghardt et al., 1983). The former case, corresponding to a small difference in dichroic signal, indicates a label that has low orientational order and negligible sensitivity to changes in the physiological state of the fiber, similar to our present results for 6′-IATR. The latter case, corresponding to a large difference in the dichroic signal, indicates a highly ordered probe that undergoes a large rotation due to a physiological state change in the fiber, similar to our present results for 5′-IATR. Consequently, the work of Tanner et al. (1992) is not comparable to our previous or present studies with 5′-IATR, and 5′-IATR continues to be a useful probe of the myosin cross-bridge in muscle fibers and in the isolated myosin preparation. Unlike many other specific probes of SH1, 5′-IATR specifically modifies this site with two probes that may be a ground-state dimer. These two probes are highly stabilized by the structure of the SH1 site.

ACKNOWLEDGMENT

The authors thank Edward Hellen from the Mayo Foundation for doing the fluorescence scanning of the gels, Paul Johnson from Molecular Probes Inc. for assistance in obtaining the purified isomers of IATR, and Andras Muhlrad from Hebrew University, Jerusalem, for helpful discussions. Computer time was furnished by the Research Computing Facility of the Mayo Foundation.

REFERENCES

Abrams, M. J., Picker, D. H., Fackler, P. H., Lock, C. J. L., Howard-Lock, H. E., Faggiani, R., Teicher, B. A., & Richmond, R. C. (1986) *Inorg. Chem. 25*, 3980–3983.

Aguirre, R., Gonsoulin, F., & Cheung, H. C. (1986) *Biochemistry 25*, 6827–6835.

Ajtai, K., & Burghardt, T. P. (1986) *Biochemistry 25*, 6203–6205.

Ajtai, K., Pótó, L., & Burghardt, T. P. (1990) *Biochemistry 29*, 7733–7741.

Bálint, M., Wolf, I., Tarcsafalvi, A., Gergely, J., & Sréter, F. (1978) *Arch. Biochem. Biophys. 190*, 793–799.

Blonski, S. (1991) *Chem. Phys. Lett. 184*, 229–234.

Borejdo, J., Putnam, S., & Morales, M. F. (1979) *Proc. Natl. Acad. Sci. U.S.A. 76*, 6346–6350.

Borejdo, J., Assulin, O., Ando, T., & Putnam, S. (1982) *J. Mol. Biol. 158*, 391–414.

Botts, J., Thomason, J. F., & Morales, M. F. (1989) *Proc. Natl. Acad. Sci. U.S.A. 86*, 2204–2208.

Burghardt, T. P., & Ajtai, K. (1986) *Biochemistry 25*, 3469–3478.

Burghardt, T. P., & Ajtai, K. (1989) *Proc. Natl. Acad. Sci. U.S.A. 26*, 5366–5370.

Burghardt, T. P., Ando, T., & Borejdo, J. (1983) *Proc. Natl. Acad. Sci. U.S.A. 80*, 7515–7519.

Burghardt, T. P., Tidswell, M., & Borejdo, J. (1984) *J. Muscle Res. Cell Motil. 5*, 657–663.

Cantor, C. R., & Schimmel, P. R. (1980) *Biophysical Chemistry Part II*, pp 392–398, Freeman, New York.
Cheng, S.-Y., & McPhie, P. (1989) *Anal. Biochem. 176*, 440–443.
Dewar, M. J., & Thiel, W. (1977) *J. Am. Chem. Soc. 99*, 4899–4907.
Dewar, M. J. S., Zoebisch, E. G., Healy, E. F., & Stewart, J. J. P. (1985) *J. Am. Chem. Soc. 107*, 3902–3909.
Elzinga, M., & Collins, J. H. (1977) *Proc. Natl. Acad. Sci. U.S.A. 74*, 4281–4284.
Frisch, M., Head-Gordon, M., Trucks, G., Foresman, J., Schlegel, H., Raghavachari, K., Robb, M., Binkley, J., Gonzalez, C., Defrees, D., Fox, D., Whiteside, R., Seeger, R., Melius, C., Baker, J., Martin, R., Kahn, L., Stewart, J., Topiol, S., & Pople, J. (1990) *Gaussian 90, Rev. H*, Gaussian Inc., Pittsburgh, PA.
Grajek, H., Zurkowska, G., Drabent, R., & Bojarski, C. (1986) *Biochim. Biophys. Acta 881*, 241–247.
Haugland, R. P. (1975) *J. Supramol. Struct. 3*, 338–347.
Hedstrom, J. F., Sedarous, S. S., & Prendergast, F. G. (1988) *Biochemistry 27*, 6203–6208.
Lakowicz, J. R. (1983) *Principles of Fluorescence Spectroscopy*, pp 112–297, Plenum Press, New York.
Longuett-Higgins, C. H., & Murrell, J. N. (1955) *Proc. Phys. Soc. (London) 68A*, 601–611.
López Arbeloa, F., Gonzales, I. I., Ojeda, P. R., & López Arbeloa, I. (1982) *J. Chem. Soc., Faraday Trans. 2 78*, 989–994.
López Arbeloa, F., López Arbeloa, T., Tapia Estévez, M. J., & López Arbeloa, I. (1991) *J. Phys. Chem. 95*, 2203–2208.
Lu, R. C., & Wong, A. (1989) *Biochemistry 28*, 4826–4829.
Mócz, G., Szilágyi, L., Chen Lu, R., Fabian, F., Bálint, M., & Gergely, J. (1984) *Eur. J. Biochem. 145*, 221–229.
Muhlrad, A., & Hozumi, T. (1982) *Proc. Natl. Acad. Sci. U.S.A. 79*, 958–962.
Rajasekharan, K. N., Mayadevi, M., Agarwal, R., & Burke, M. (1990) *Biochemistry 29*, 3006–3013.
Ridley, J., & Zerner, M. (1973) *Theor. Chem. Acta (Berlin) 32*, 111–133.
Rohatgi, K. K., & Mukhopadhyay, A. K. (1971) *Photochem. Photobiol. 14*, 551–559.
Selwyn, J., & Steinfeld, J. I. (1972) *J. Phys. Chem. 76*, 762–774.
Tanner, J. W., Thomas, D. D., & Goldman, Y. E. (1992) *J. Mol. Biol. 223*, 185–203.
Thorn, D. L., & Fultz, W. C. (1989) *J. Phys. Chem. 93*, 1234–1243.
Tong, S. W., & Elzinga, M. (1983) *J. Biol. Chem. 258*, 13100–13110.
Tonomura, Y., Appel, P., & Morales, M. F. (1966) *Biochemistry 5*, 515–521.
Weeds, A., & Taylor, R. S. (1975) *Nature (London) 257*, 54–56.